Astron. Astrophys. 16–32 (1987)

ASTRONOMY AND ASTROPHYSICS

Fragmenting the Universe

I. Statistics of two-dimensional Voronoi foams

V. Icke and R. van de Weygaert

Sterrewacht Leiden, Postbus 9513, NL-2300 RA Leiden, The Netherlands

Received November 27, 1986; accepted January 22, 1987

Summary. We present a Monte Carlo study of the matter distribution in a kinematical model of superclustering in the Universe. It has been shown (Centrella and Melott, 1983; Icke, 1984) that the regions of lower than average density in the early Universe become more and more spherical as time goes by. Thus, the large scale morphology of the high-density baryonic material in the Universe, consisting of "clusters" in the form of pancakes, filaments, and nodes is obtained when matter streams away from a distribution of low-density expansion centres ("nuclei") and collects in the interstices of a close packing of spheres.

This naturally leads to a partitioning of space generated by a process known as *Voronoi tessellation*. We have studied the statistical properties of specific instances of these tessellations, which we call Voronoi foams, for several model distributions of expansion centres. We derive the statistical properties of the regions where baryonic matter accumulates, and of the voids between the galaxies. These can be compared with observations, leading to indirect constraints on the initial spectrum of the density perturbations that produced the matter distribution we observe today.

In this article we give numerical results on two-dimensional Voronoi foams and several of their statistical properties in the case of correlated as well as anticorrelated distributions of nuclei, together with a description of the algorithm used for generating these foams from a given distribution of nuclei. The properties of three-dimensional Voronoi foams will be presented in a subsequent article.

The appearance of a Voronoi foam closely resembles the mass distribution found in numerical hydrodynamic experiments, and the bubble structure observed in the galaxy distribution. Concerning the statistical properties of the Voronoi cells, we conclude that the most promising way to discriminate between several distributions of nuclei is looking at the variance of the angles between filaments of galaxies. For example, a notable finding is that the variance of the angle between Voronoi cell walls is about a factor two smaller than the variance of the angle between randomly placed walls. This large factor should be easy to discern in galaxy statistics, and will be useful in discriminating between a "cell" structure of the Universe and a random distribution of luminous matter.

The distribution of angles in a Voronoi foam generated by a completely random distribution of nuclei is known analytically. In the Poissonian limit, our numerical results agree precisely with the analytical expressions.

Key words: cosmology – galaxies: clusters of – mathematical methods

Send offprint requests to: V. Icke

1. Introduction

1.1. General outline

Because we intend this article to be the first in a series of investigations of the large scale structure of our Universe, we present an introduction that is a little longer than usual, in order to outline the various ramifications we hope to study.

Theoretical predictions of highly anisotropic structures in the Universe (Oort, 1970; Zel'dovich, 1970; Icke, 1972, 1973) have been confirmed by extensive observations of the large scale distribution of galaxies (Einasto et al., 1980; Zel'dovich et al., 1983; cf. also Oort, 1983, and references therein). The analytic estimates referred to above have been confirmed, extended and refined by numerical calculations of the formation of structure in the early Universe (Centrella and Melott, 1983; Klypin and Shandarin, 1983; Melott, 1983; Shapiro et al., 1983; Frenk et al., 1983; Bond et al., 1984). Although there is doubt about the reliability of some galaxy counts (De Lapparent et al., 1986), it would appear that the reality of the sponge-like distribution of luminous matter is well established (Oort, 1983; De Lapparent et al., 1986). Filaments in redshift sections might also be due to the type of "velocity crowding" cusps that plague galactic (l, v)-diagrams (Burton, 1976; Kaiser, 1987), but this effect cannot explain the evident filaments that are seen projected in the sky. We will therefore proceed on the assumption that the void-and-filament mass distribution is typical of the Universe on scales above, say, 15 megaparsec (using a Hubble parameter of $75\,\mathrm{km\,s^{-1}\,Mpc^{-1}}$).

The statistical properties of the galaxy distribution calculated in the numerical models (Centrella and Melott, 1983; Klypin and Shandarin, 1983) should be compared with those of the actual galaxy statistics of our patch of the Universe. However, these calculations suffer somewhat from resolution problems, and in any case they are very expensive in computer time. It may therefore be useful to see if simpler models can help to narrow down the parameter space of the actual mass distribution. To this

end, it is very helpful that it can be shown that the low-density regions, or "voids", become more and more spherical as time goes by (Icke, 1984; see Sect. 1.2 below).

This leads to a picture of structure formation that is fully in accord with the sponge structure (Gott et al., 1986) of the observed galaxy distribution: we can imagine a collection of expansion centres, i.e. areas where the cosmic expansion goes a little faster than the average Hubble speed, from which matter flows away and collects on the interfaces of a population of spheres that surround the expansion centres. This gives rise to three topologically distinct mass aggregates: contact surfaces (pancakes), which divide adjacent expanding bubbles; filaments, where those pancakes intersect; and nodes, formed by the intersection of the filaments. Not only is this interesting because it gives a basis for comparison with observations, but also it suggests a way out of the apparent conflict between the small-scale statistical properties of the galaxy distribution (as seen in the two point correlation function) and the epoch of formation of the larger structures. Because in the Voronoi foam (see Sect. 2.1 for definition of terms) matter streams towards the pancakes along one spatial dimension, these grow most slowly; the filaments grow by accretion in two dimensions, and thus their density increases faster; and nodes acquire matter from all directions, and therefore grow fastest. Thus, it is possible that the basic foam structure *does* form before galaxies, but that galaxies form before the pancakes have become very evident. In fact, it may be that the pancakes become hardly noticeable at all, so that the foam structure is mostly visible in the distribution of filaments and nodes.

In this scenario, the first generation of stellar systems forms in the nodes. If these are associated with quasars, the clustering properties of the latter are expected to be different from those of galaxies, which are assumed to form in the filaments as well as in the nodes (only later; see Sect. 5). The two point correlation is then presumably established by the comparatively small-scale process of interactions among individual stellar systems, which dynamically are known to behave as very inelastic bodies (see Sect. 1.3).

In this article, we present the results of a Monte Carlo study of the statistical properties of such a cellular distribution in two dimensions. Our aim is, to provide a family of statistical distributions, based on the dynamic properties of the evolution of voids (namely that they become more spherical as they become less dense in the course of time); observations can then determine which, if any, member of this family most resembles the actual mass distribution of the Universe. We can thus put constraints on the properties of the perturbations from which the voids developed. The algorithms, computer code, and comprehensive results will be published separately; work on the three-dimensional case is in progress. The special case of a Poissonian cell distribution was originally applied by Kiang (1966) to the problem of fragmentation during star formation.

We expect that our results have a wider application than in cosmology alone; possible areas include other fragmentation scenarios, such as star formation, the statistics of cellular structure in turbulent atmospheres, or in the interstellar "cirrus". Furthermore, the "minimal triangulation" properties of the Delaunay triangles associated with the Voronoi tessellation suggests that it would be a very useful instrument for the plotting of contours of an irregularly sampled function (Kendall, 1971). Applications of Voronoi tessellations include such diverse fields as molecular physics, biochemistry, materials science, physical chemistry, geology, the study of liquids and amorphous solids (e.g. structureal studies of metallic glasses and the glass transition) and even the study of the growth of weeds in a field of crop plants (Fischer and Miles, 1973).

1.2. The bubble theorem

It was shown by Lynden-Bell (1964) and by Lin et al. (1965) that a homogeneous ellipsoidal dust cloud collapses in such a way that any slight departure from sphericity is systematically magnified during the evolution of the cloud. Subsequently, Icke (1972; see also Fig. 5 in Oort, 1970) extended this result and argued that all large-scale density excesses in the Universe will thus become filamentary, leading to the formation of very elongated clusters of galaxies. Some evidence for these structures was seen in the Virgo and Perseus clusters (Icke, 1972), but the redshift data were at that time insufficient to establish the presence of the expected systematic large-scale streaming (Icke, 1973).

By a simple inversion of Lynden-Bell's (1964) argument, it can be shown that the reverse of the above holds true too. A void can be considered as a negative-density region in an average background of positive density, so that, when the condensations collapse, the voids expand. This seems like a useless tautology, until one realize that a reversal of the sign of the density means that *as the void becomes bigger, its asphericities will gradually disappear* (Icke, 1984). The effects of this "bubble theorem" show up clearly in the numerical work of Centrella and Melott (1983) and of Bertschinger (1985b). The virtue of the above is, that precisely those regions which represent most of the volume of the Universe have the simplest geometrical shape. Therefore, it would seem to be sensible to construct a model of the mass distribution in the Universe based on such simple entities. One may then think of the condensations as occupying the interstitial spaces of a close packing of expanding spheres of different sizes.

1.3. "Large" and "small" structures

Theories of the formation of structure in the Universe are usually rather vague about what determines the shape and spectrum of the density deviations, and about precisely what is meant by "large" and "small" structure. Some general mass scales and fluctuation spectra have been identified (e.g. Rees, 1971; Efstathiou and Silk, 1983), but these often depend on the details of the thermal history of the Universe or on the intricacies of hypothetical "grand unified theories" of relativistic quantum fields. We will take a rather more pedestrian view, and identify our mass scales as follows.

Implicit in our scenario is the assumption that galaxies form later than their parent clusters, or at least at an epoch when the cluster collapse was well under way (Oort, 1970; Icke, 1973; Oort, 1983). This allows us to estimate the minimum size of the Voronoi cells that will be considered in what follows. If a cell wall collapses, the Kelvin-Helmholtz radiation that is thereby liberated must not be absorbed by another wall, or else the added energy would prevent this wall from collapsing in its turn. Accordingly, it is plausible that the light travel time across a Voronoi cell must exceed the collapse time of galaxies in a cell wall. The corresponding cell size is then roughly 10 Mpc; if this occurred at a redshift of about 5, the present cell scale would be of the order of 50 Mpc, with a corresponding velocity scale of some 4000 km s^{-1}. These numbers then determine what will be called "large scale" in the remainder of this work.

As to the "small' scale, this is clearly determined by the length scale on which the motion of galaxies is influenced by the fact that they are not elastic point particles. In some work, it is assumed that galaxies and gas form a two-component system, where one

(the gas) is collision dominated, whereas the other (the galaxies) is collisionless. This would be a good approximation for a mixture of stars and gas under typical galactic circumstances, but it is inadequate for galaxies and gas. After all, galaxies have an immense number of internal degrees of freedom, which are easily excited in encounters (Toomre and Toomre, 1972). Thus, it seems plausible to define any distance as small if a galaxy collision at that distance is likely to produce significant tidal distortion. If both galaxies have mass M, the tidal acceleration A across a galactic diameter $2R$ is equal to $4GMRr^{-3}$, if r is the distance between the galaxies. The encounter induces an excess speed Δv in about one galactic year $2\pi R/v$, where v is the circular speed at R, and $\Delta v \approx 8\pi v(R/r)^3$. If the induced velocity change exceeds 10 % of the galactic rotation speed, noticeable tides can be expected, so that any distances less than $r = R(80\pi)^{1/3}$ can be called "small".

This distance is 200 kpc or so, or several hundred times less than our "large" scale. This justifies our use of the large scale cells without explicit reference to the behaviour of the galaxies in their walls. However, it clearly shows the need for incorporating the galaxies as soft particles in calculations of the transverse cell wall structure (we intend to do this in our future work). Moreover, the sizable ratio between large and small scales indicates the difficulty of properly resolving the collapsing structures in numerical simulations (Centrella and Melott, 1983, 1985; Klypin and Shandarin, 1983). We suspect that the filamentary clusters are transversely virialized on small scales, and that the two point correlation of galaxies, extensively studies by Peebles and collaborators (Peebles, 1980, and references therein), finds its origin in the dissipational behaviour of galaxies in the small scale encounters that produce this virialization. If that view turns out to be correct, the two point correlation would be a "final touch" to the evolution of the structure of the Universe, mostly unrelated to the events on a large scale.

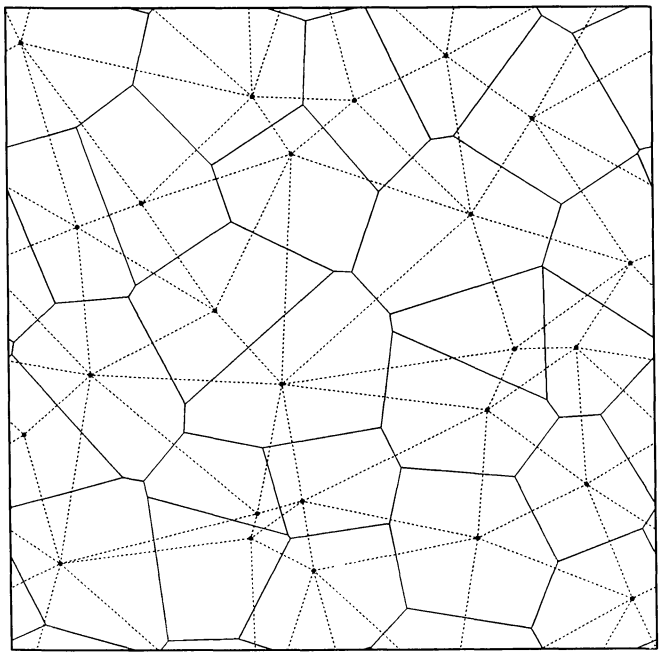

Fig. 1. Example of a Voronoi tessellation (thick solid lines) and its corresponding Delaunay triangulation (thin solid lines) with periodic boundary conditions. The points where several lines of the Delaunay triangles meet are the nuclei of the Voronoi tessellation; the points where several lines of the Voronoi tessellation meet are the circumcentres of the corresponding Delaunay triangles. Note that the circumcentre can lie outside its Delaunay triangle

2. The Voronoi problem

2.1. The tessellation

Consider a box of finite size in N-dimensional space (in our case $N=2$ or 3), in which are distributed a fixed number of points according to some statistical process (e.g. Poissonian). Suppose that each of these points is the centre of a spherical expanding bubble. If all the bubbles begin their expansion at the same time and at the same rate, the bubbles will come together on planes that orthogonally bisect the lines connecting the expansion centres (in accordance with accepted terminology, we will call such a centre a *nucleus*). The bisecting planes intersect each other, thereby generating lines; these lines in turn intersect and form a network. In this way, each nucleus is enclosed by a set of plane N-1-dimensional planes, encompassing a convex cell containing the nucleus. Accordingly, the distribution of nuclei generates a unique tiling of N-space, the *Voronoi tessellation* (Voronoi, 1908).

The points of a Voronoi cell all share the property that they are closer to the cell's nucleus than to any other (Fig. 1). Present knowledge about Voronoi tessellations stems from the pioneering works of Meyering (1953), Gilbert (1962) and Miles (1970). Only one distribution function (i.e. the distribution function of angles between adjacent lines, see Sect. 3.2 and Fig. 9) and only a limited number of statistical moments (e.g. expectation values) of Voronoi tessellations are known analytically in the case of a homogeneous Poissonian point distribution (see Tables 1 and 2).

Apparently, this mathematical construct is a wheel that keeps being reinvented, and so it has acquired a set of alternative names: Dirichlet regions, Voronoi polygons/polyhedra, Wigner-Seitz cells, or Thiessen figures. In fact, the senior author was guilty of the N^{th} reinvention, but his junior uncovered the vast amount of literature on Voronoi tessellations via the work of Kiang (1966). We will use the name *Voronoi tessellation* for the division process; a particular realization of this process (i.e. a subdivision of N-space according to the Voronoi prescription for a particular set of nuclei) we will call a *Voronoi foam*. In the calculations presented below, we will restrict ourselves to $N=2$.

For the homogeneous planar Poisson point process the exact known expectation values for a Voronoi cell are given in Table 1 (Miles, 1970). The corresponding exact moments for a Voronoi polyhedron produced by a homogeneous three dimensional Poisson point process are shown in Table 2 (Meyering, 1953; Miles, 1972). Other properties of Voronoi figures have been found by Monte Carlo techniques, generating a large number of statistically independent tessellations and thereby determining experimentally the distribution functions of, say, the lengths of the tile edges, the angles between adjacent edges, or the tile surface. We will do the same here, with a view toward comparing these statistical measures to those inferred from the actual galaxy distribution. We will not restrict ourselves to Poissonian nuclei (the only case extensively treated in the mathematical literature), but consider correlated and anticorrelated nuclei as well.

Eventually, we will compare the resulting Voronoi foams with the actual distribution of galaxies; this is made possible by automated analysis of large samples of galaxies (Rhee and

Table 1. Exactly known moments for a two-dimensional Voronoi cell in the case of a homogeneous Poisson point process. Here ϱ is the "intensity" of the process, i.e. the number of points per unit volume in N-space

Quantity	Moment
1. Number of vertices	$E(N)=6$
2. Area	$E(A)=1/\varrho$
3. Perimeter	$E(S)=4/\sqrt{\varrho}$

Table 2. Exactly known moments for a three-dimensional Voronoi polyhedron in the case of a homogeneous poisson point process

Quantity	Exact	Numerical
1. Volume		
$E(V)$	$1/\varrho$	$1/\varrho$
2. Surface area		
$E(S)$	$(256\pi/3)^{1/3}\,\Gamma(5/3)\,\varrho^{-2/3}$	$5.821\,\varrho^{-2/3}$
3. Edge length		
$E(L_1)$	$\{4^{5/3}\pi^{5/3}\,\Gamma(1/3)\}/\{3^{2/3}5\varrho^{1/3}\}$	$17.50\,\varrho^{-1/3}$
4. Number of edges		
$E(N_1)$	$144\pi^2/35$	40.61
5. Number of faces		
$E(N_2)$	$(48\pi^2/35)+2$	15.54
6. Number of sections per unit area cut by a plane		
$E(M_1)$	$\{4^{2/3}\pi^{5/2}\,\Gamma(1/3)\}/\{3^{5/3}5\varrho^{1/3}\}$	$1.458\,\varrho^{-1/3}$

Katgert, 1987). By finding a connection between the distribution (of (say) edge lengths and the amount of (anti)correlation of the nuclei, we may be able to place some limits on the latter by comparing it with observations. This would enable us to "observe what is not there", i.e. the statistical properties of the voids between the galaxies, and indirectly the spectrum of perturbations that led to the formation of large scale structure in the Universe.

2.2. *The algorithm*

From the above, it follows that the algotithm for the Voronoi tessellation must proceed as follows:

(1) Pick a distribution of nuclei;

(2) Prescribe boundary conditions;

(3) For each nucleus, construct the circumference of its Voronoi tile, which encompasses all points that lie closer to the given nucleus than to any other.

In step (1), the distributions we use can be correlated, uncorrelated (Poissonian), or anticorrelated. Because there is an infinity of possibilities for (anti)correlation, we had to make a choice. In order to explore the most characteristic possibilities we will proceed as follows. We take a two-dimensional grid of 25×25 arbitrary length units, in which we place 100 nuclei. In the case of anticorrelation the grid is subdivided in 25 grids of 5×5; in each subgrid four nuclei are placed in such a way that the minimum distance to any other nucleus in the 25×25 grid is larger than a prescribed value, denoted by δ, which may be called the "anticorrelation parameter". We ran 18 different δ's, from $\delta=0.0$ to $\delta=1.7$, in steps of 0.1; $\delta=0.0$ is the most random distribution (i.e. it most closely resembles a Poissonian distribution). Examples for $\delta=1.7$, $\delta=1.0$ and $\delta=0.0$ are shown in Fig. 2a, b, c.

We also explored a correlated process. In this case, the first nucleus is placed at random, and each subsequent nucleus is placed with respect to its predecessor according to the following prescription:

$$r=-\lambda\log R[0,1]$$
$$\phi=R[0,2\pi].$$

Here r is the distance to the preceding nucleus, while ϕ marks the direction with respect to the x-axis; $R[a,b]$ is a random number between a and b. The number λ will be called the *correlation parameter*. If λ is small (i.e. $\lambda\lesssim2.0$) we have very correlated distributions (Fig. 2f). As far as we know, these bear little resemblance to physical reality as seen in the actual distribution of low- and high-density regions in the early Universe. If λ lies between ≈2.0 and ≈7.0 (Fig. 2e), we obtain a middle correlated distribution; above $\lambda\approx7.0$ (Fig. 2d), the correlation becomes very weak. We ran 40 different λ's; from $\lambda=0.2$ to $\lambda=4.0$ in steps of 0.2 and from 4.4 to 12.0 in steps of 0.4.

The above two processes were chosen mostly for convenience. For the benefit of those who want to explore Voronoi foams centered on other distributions of nuclei, we will publish our algorithm and FORTRAN code elsewhere, together with more statistical details than are given here. Our processes become poissonian only in the asymptotic limit $\delta\downarrow0$ and $\lambda\to\infty$.

In step (2), we prescribe toroidal boundary conditions: our sample of a two-dimensional universe is square, and the opposing edges are identified with each other.

In step (3) there ar two possibilities. The first one is recursive, has a finite resolution, and can be generally applied. We subdivide our square (e.g. into four quarters, but the actual number can be chosen freely for optimal convergence); determine of each corner of a small square where the nearest expansion centre is; and if not all four corners belong to the same centre, apply the same subdivision to the small square. We will be using this method in the more difficult case of unequal expansion velocities, which is known in the literature as the Johnson-Mehl subdivision of space (Johnson and Mehl, 1939). A comparable method was used by Kiang (1966), who determined the Voronoi tessellation of a random distribution of 80 nuclei by determining the nearest nucleus for each point out of a grid consisting of 6400 points. The second method is geometric, exact, and is economic only in the case of equal expansion velocities.

The essence of the method we used for constructing a Voronoi foam is described by Tanemura et al. (1983) in the case of three dimensions. Other algorithms, which turn out to be less efficient, can also be found in the literature (Kiang, 1966; Green and Sibson, 1978; Brostow and Dussault, 1978; Finney, 1979)[1]. Our method works as follows.

Consider a distribution of nuclei in a plane. We take any nucleus and label it N_1, and determine the Voronoi cell of nucleus N_1; this step is repeated for each nucleus in the grid.

[1] In fact, we discovered the article of Kiang (1966) and, via this work, a host of further articles, after we had already written and tested our own program.

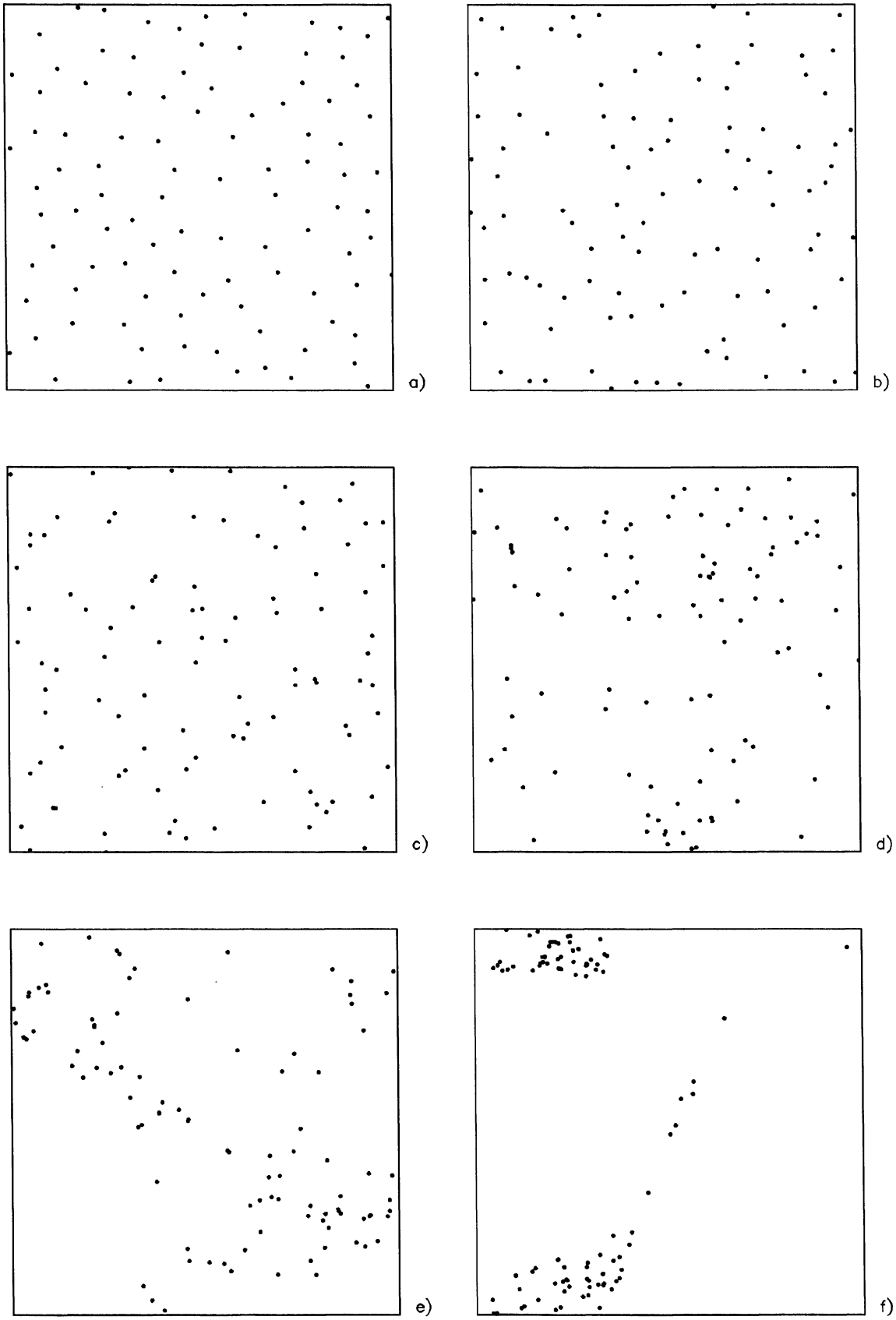

Fig. 2a–f. Six examples of the distribution of nuclei (expansion centres) according to our prescription of correlation and anticorrelation. Panels **a** through **c** are anticorrelated distributions: **a** very anticorrelated (quasi-crystalline) ($\delta = 1.7$); **b** mildly anticorrelated ($\delta = 1.0$); **c** quasi-Poissonian ($\delta = 0.0$). Panels **d** through **f** are correlated distributions: **d** weakly correlated ($\lambda = 7.6$); **e** middly correlated ($\lambda = 3.2$); **f** strongly correlated ($\lambda = 1.0$)

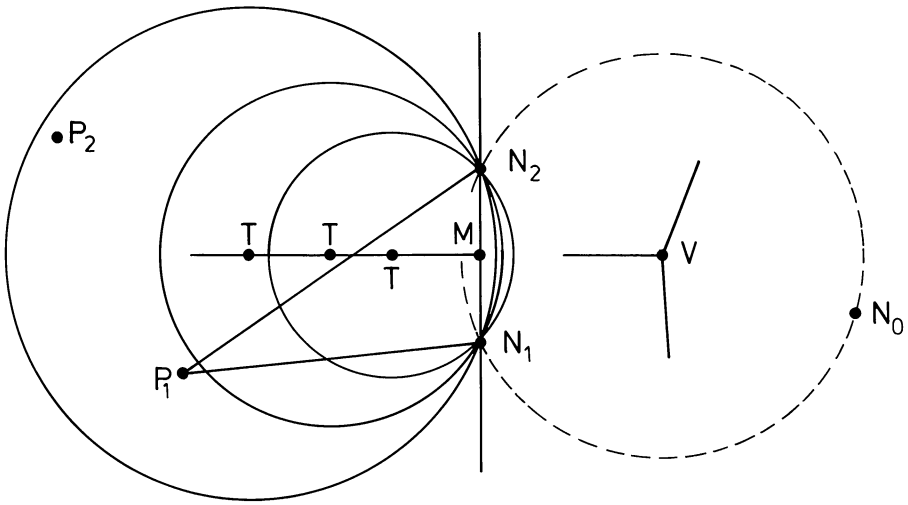

Fig. 3. The construction of a new Delaunay triangle from two known nuclei (N_1 and N_2) by searching for a new nucleus N_3 such that (N_1, N_2, N_3) forms a triangle whose circumsphere doesn't contain any other nucleus (see text). The points N_0, N_1, N_2 form a Delaunay triangle obtained in a previous search; within the (dashed) circumcircle of (N_0, N_1, N_2) is shown corresponding Voronoi vertex V, and stubs of the Voronoi cell walls. On the left hand side of the diagram, the T are a sequence of trial points, the third of which produces a circle that encompasses two nuclei, P_1 and P_2. Because the radius of the circumcircle of (N_1, N_2, P_1) is smaller than that of (N_1, N_2, P_2), the point $P_1 = N_3$, i.e. the third corner of the Delaunay triangle. Thus, the circumcentre of (N_1, N_2, P_1) is the next Voronoi vertex, which, if connected with V, produces a complete Voronoi cell wall

The determination of a Voronoi cell consists of a sequential search for all so-called *Delaunay triangles*, which are the triangles having three nuclei as vertices and a circumscribing circle that contains no other nuclei (Fig. 1). A property of a Delaunay triangle is that the centre of the circumscribing circle is a vertex of the Voronoi foam (Fig. 1), because by definition each triple of nuclei that generates a Voronoi vertex is equidistant from that vertex and is the nearest triple of nuclei to that vertex. If we have found all Delaunay triangles having N_1 as a corner, in the right order, we can construct the Voronoi cell belonging to N_1 by joining the circumcentres of the Delaunay triangles.

Our program stars with looking for the nearest neighbour nucleus of N_1 and labeling it N_2. The plane that perpendicularly bisects the line between N_1 and N_2 is a wall of a Voronoi cell (a line, in two dimensions). Now we look for a third nucleus N_3, such that (N_1, N_2, N_3) forms a Delaunay triangle. Finding that nucleus is done by using the property that the circumscribing circle of (N_1, N_2, N_3) is empty; if there is another nucleus inside the circle, it is nearer to the circumcentre than N_1, N_2, or N_3, and therefore the circumcentre cannot be a vertex in the Voronoi tessellation. The nucleus N_3 is found by starting at the midpoint M between N_1 and N_2 and moving a trial point T outward along the perpendicular bisector. We always move in a counterclockwise direction along the bisector, i.e. we "turn left" as seen from N_1. This direction is arbitrary, but it must be adhered to once the choice is made. The search begins with a point T such that $TM = MN_1$. Around T a circle is drawn with a radius equal to the distance TN_1 (and TN_2). If no nuclei are found in that circle, we move further outward to a new T on the bisector and repeat the same step, at each such move the distance TN_1 is increased by a fixed factor ($\sqrt{2}$ in our calculations) in order to speed up the search process; as soon as we find nuclei inside the circle we calculate for each such nucleus (say P_i) the circumcentre of the triangle (N_1, N_2, P_i), followed by the determination of the distance D_i of that circumcentre to the midpoint between N_1 and N_2. The nucleus N_3 is that nucleus P_i for which D_i is minimal (see Fig. 3); consequently, (N_1, N_2, P_i) is a Delauney triangle. The circumcentre found is the first vertex of the Voronoi polygon centered on N_1. Then we move along the perpendicular bisector between N_1 and N_3 (again in counterclockwise direction) and, in like manner, find a fourth nucleus N_4 which defines the second vertex of the polygon (circumcentre of triangle (N_1, N_3, N_4). This procedure is repeated until we are back where we started, and have completed the Voronoi polygon associated with N_1. With the proper bookkeeping to avoid duplications, the same procesure is applied to all the other nuclei, and thereby the tessellation is completed. The process is shown schematically in Fig. 3.

The extension to three dimensions is obvious: four nuclei form a Delaunay tetrahedron if it has a circumsphere that has no other nuclei inside. The centre of the circumsphere is a Voronoi vertex.

It is clear that at a generic Voronoi vertex in two dimensions, three cells meet; however, if by chance a vertex has four or more Voronoi polygons in common, i.e. two contiguous Delaunay triangles have the same circumcircle, the vertex is said to be degenerate. Although such degeneracy will not occur in reality, we have for the sake of safety tested our programs on degenerate cases (e.g. a square grid of nuclei), and found that these are treated properly by our algorithm.

The literature is replete with illustrations of poissonian Voronoi foams (Kiang, 1966; Green and Sibson, 1978; Sibson, 1980; Miles and Maillardet, 1982). However, we wanted to look especially at the change of the properties of the tessellations as a function of the distribution of the nuclei. To give an idea of the resulting patterns, six Voronoi foams, corresponding with the distributions of nuclei from highly correlated to highly anti-correlated (Fig. 2), are shown in Fig. 4.

Although it is clear that the Voronoi tessellation corresponding to highly, and even mildly, correlated distributions of nuclei (Fig. 2f) bear no resemblance to the observed cell structure of the Universe, the anticorrelated and weakly correlated distributions do resemble the large scale structure of the Universe (cf. De Lapparent et al., 1986) and the structure seen in numerical simulations (e.g. Centrella and Melott, 1983). There are two ways we can interpret the two dimensional Voronoi foams shown in Fig. 4. First, we can consider them as a slice of the Universe (as in De Lapparent et al., 1986); alternatively, we can consider the foam as a projection on the sky of the galaxy distribution, as seen in a map of the famous Shane-Wirtanen counts (Shane and Wirtanen, 1967; Seldner et al., 1977). Although our two-dimensional pictures are not yet the projection of three-dimensional Voronoi foams, we can make a preliminary comparison between our results and the actual sky because the galaxy counts are magnitude limited and, consequently, encompass a finite slice in depth. If that

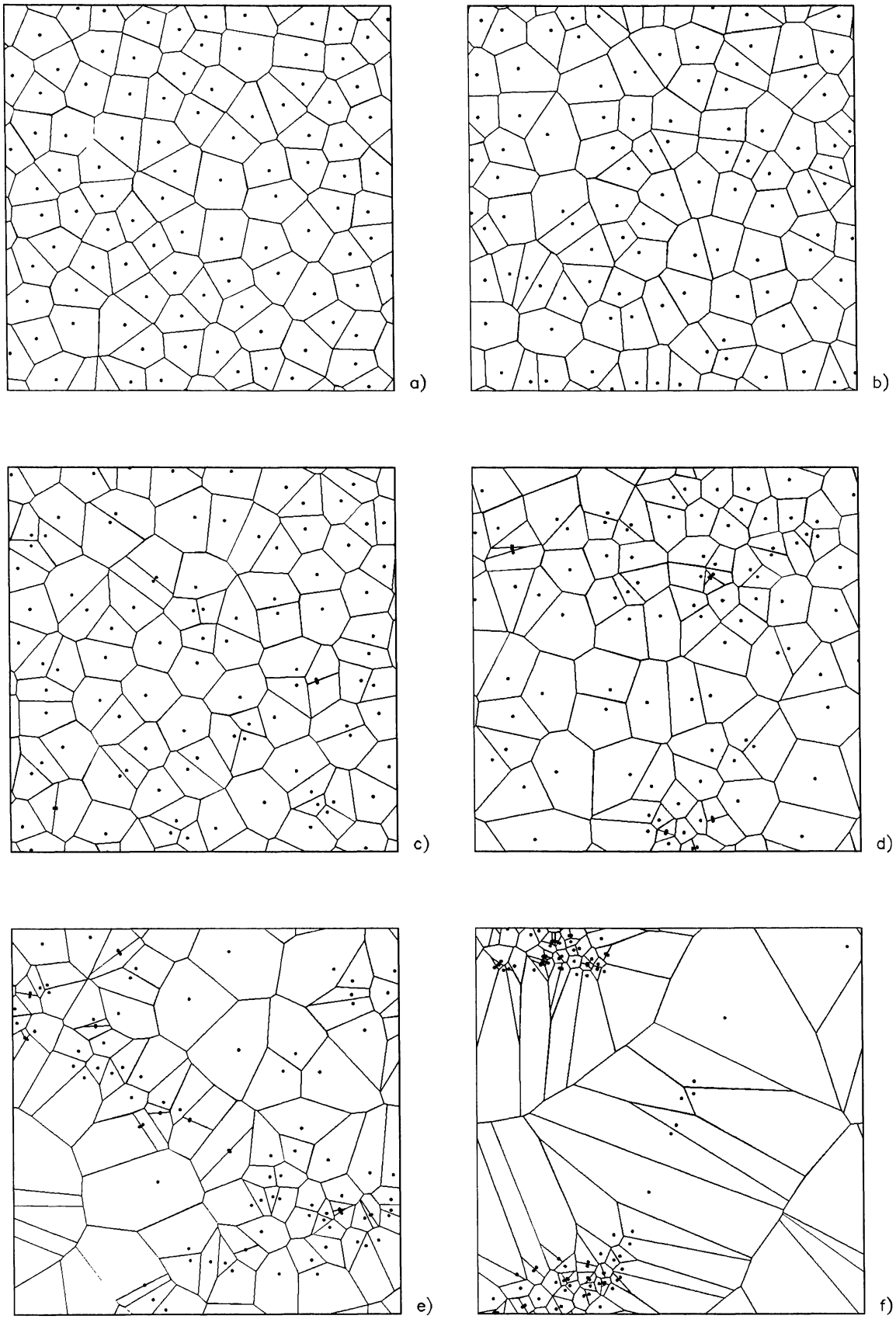

Fig. 4a–f. Six examples of Voronoi foams. The cases **a** through **f** correspond with the similarly numbered distributions of nuclei a) through f) in Fig. 2

depth is of the order of the cell size, the two dimensional results should be a first approximation of reality. The limiting photographic magnitude of the Shane-Wirtanen counts is 19^m. Assuming an absolute photographic magnitude for a typical galaxy of -18^m, this corresponds to a depth of 250 Mpc. The typical size of a void could easily be 50 Mpc (Oort, 1983; De Lapparent et al., 1986), which means a depth of five Voronoi cells; a projection of a shell with a width of this number of cells will probably still look much like a two-dimensional cell structure. We intend to test this when we have produced our three-dimensional Voronoi algorithm.

It must be emphasized that the Voronoi foams (Fig. 4) do not give the density distribution of galaxies; they represent, as it were, the skeleton around which the galaxies will assemble during the evolution of the Universe. Matter first arrives in the pancakes, followed by the filaments and lastly the nodes; however, the density at the nodes grows much faster than at the filaments, whose density, in turn, grows faster than the density at the pancakes (Icke, 1984). In advanced stages of collapse of the filaments we must also expect streaming of matter from the pancakes and the filaments towards the nodes so that it is possible that only a relatively small number of galaxies will exist in the pancakes, giving rise to a sponge-like picture of the galaxy distribution (Gott et al., 1986). It would be very interesting to calculate the density evolution of our Voronoi model and the topological properties of the resulting low- and high-density regions, after the manner indicated by these authors.

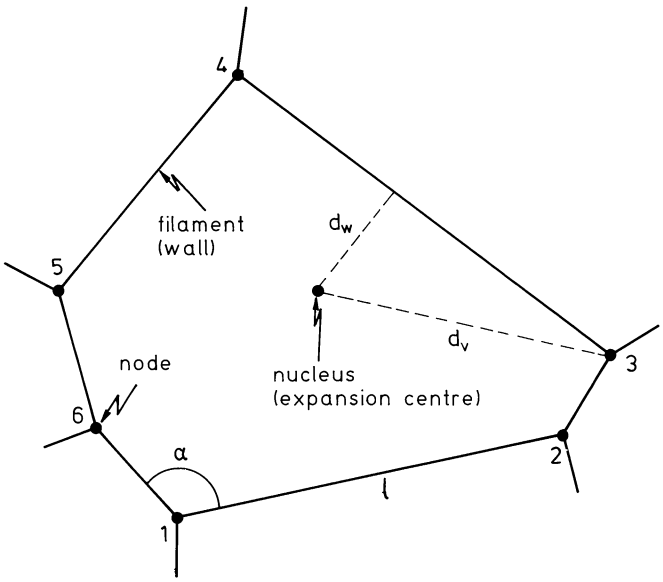

Fig. 5. Identification of the four quantities which were calculated in each Voronoi cell: l_i: length of wall i; α: angle between two walls meeting at a vertex; d_V: distance between the nucleus and a vertex: d_W: distance between the nucleus and a wall (note that the projection of the nucleus doesn't necessarily lie on the wall). Other quantities which were calculated are the number of vertices of the cell (here 6), the circumference, and the area

3. The statistical properties of Voronoi foams

3.1. Quantities derived from the Monte Carlo simulations

Each Voronoi foam was analyzed statistically, by determining for each cell: a) the circumference; b) the area; c) the number of vertices; d) the length of each wall; e) the angle between each pair of neighbouring walls; f) the distance between the centre and each vertex; g) the perpendicular distance between the centre and each wall (Fig. 5). This produced seven sets $\{A_i\}$ of cell properties. We calculated, over the whole foam of $K=100$ Voronoi cells, 1) the mean of each set $\{A_i\}$, $\overline{A}=\sum_{i=1}^{L} A_i/L$; 2) the variance $\delta_A=\left\{\sum_{i=1}^{L}(A_i-\overline{A})^2/(L-1)\right\}^{1/2}$; 3) the maximum; 4) the minimum. For each correlation- and anticorrelation parameter λ resp. δ we initiated $M=26$ different distributions of nuclei and calculated the corresponding Voronoi foams. For each foam, the four quantities mentioned above were obtained, producing four sets $\{B_j\}$ for each cell property. The mean $\overline{B}=\sum_{j=1}^{M} B_j/M$ and its variance $\delta_B=\left\{\sum_{j=1}^{M}(B_j-\overline{B})^2/M(M-1)\right\}^{1/2}$ were determined. In cases a) through c), L is the number of cells in the foam (equal to $K=100$ in the simulations presented here). In case e), L is the number of angles in the foam, i.e. three times the number of vertices. In cases d), f), and g), L is the number of walls, i.e. 3/2 times the number of vertices. The values $\overline{B}$ were plotted as a function of λ and δ. The variance δ_B was indicated with an error bar at each point. Representative examples of such plots are shown in Fig. 6.

By this procedure, we hoped to identify those quantities which are most sensitive to correlation or anticorrelation of the nuclei. From these, we may be able to derive information about the distribution of the expansion centres in the Universe, which are of course invisible, but which ought to contain fossil information about the fluctuation spectrum from which the observed structures of luminous matter arose.

Furthermore, if the Voronoi cells got their initial push from expansion that was initiated by early vigorous phases of galaxy formation (Ostriker and Cowie, 1981; Ikeuchi, 1981) one ought to expect that the expansion centres lie near these initially active objects. Then these centres become interesting regions for study, because the cinders of the first generations of active stellar systems might still be found there.

Quantities like the mean and the variance of cell properties give an impression of the effect of correlation or anticorrelation on the foam structure. However, the distribution of other quantities may be more sensitive to λ and δ. In order to identify these, we made histograms of the cell properties a) through g) (Fig. 7a through g). Each histogram contained the data of the entire Monte Carlo sample of 26 foams, for a given value of λ or δ. The graphs (except in case c) were constructed by binning the data such that each interval contains the same number of points. The bin width is equal to the largest value of any point contained in it, minus the largest value of the points in the former bin. The height of the histogram at each bin is equal to the relative frequency, given by $f_i=n_i/N_{\text{tot}}\,b_i$. Here n_i is the number of points in the i^{th} bin, N_{tot} is the total number of points contained in the 26 tessellations, and b_i is the width of the i^{th} bin. If the number of points per bin is chosen carefully, this procedure gives proper resolution and a constant scatter per bin.

3.2. Qualitative behaviour of the derived quantities

First, let us consider how the frequency distributions of the derived quantities vary as a function of the (anti)correlation of the

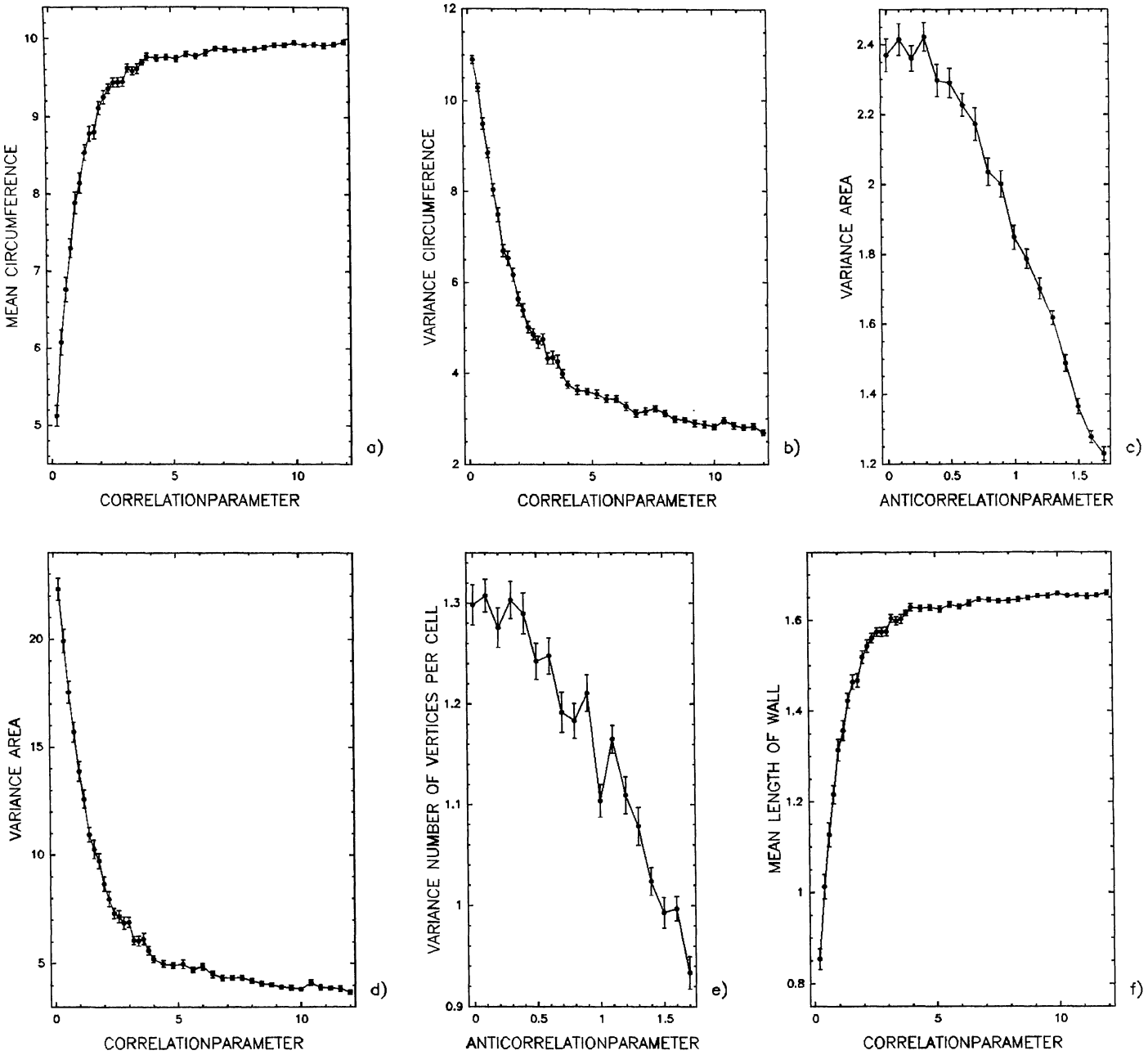

Fig. 6a–i. Plots of the mean and the variance of several quantities of the Voronoi tessellation as a function of the correlation parameter (λ) resp. anticorrelation parameter (δ). **a** The mean circumference as a function of λ. **b** The variance of the circumference as a function of λ. **c** The variance of the area as a function of δ. **d** The same as **c**) but as a function of λ. **e** The variance of the number of vertices per cell as a function of δ. **f** The mean length of a wall as a function of λ. **g** The variance of the length of a wall as a function of δ. **h** The variance of the angle at a vertex as a function of δ. **i** The same as **h**, but as function of λ. Each point in the plot is the result of 26 different distributions of nuclei with that particular correlation or anticorrelation parameter. The error bars give the variance of the quantity as calculated from these 26 distributions (see text, Sect. 3.1)

nuclei. The least variable is the number of vertices per cell (Fig. 7c). This is surely due to the fact that the average number of vertices per nucleus is constant, independent of the statistical distribution of the nuclei. Accordingly, the average number of vertices per cell is the same as in the crystalline grid [2] (which is a special case of a Voronoi foam), namely six. Strongly correlated nuclei generate a low and long tail on the distribution, but this will be very difficult to observe in reality; moreover, the pattern of inhomogeneities of the galaxy distribution in the sky is obviously not generated by a very strongly correlated set of expansion centres. This by itself is a useful datum, but comparison with other derived quantities of the Voronoi foam will be seen to be preferable for comparison between the statistical models and the actual distribution.

[2] This is one of the reasons that the hexagonal distribution used by Hoffman et al. (1983) closely resembles our poissonian Voronoi foam

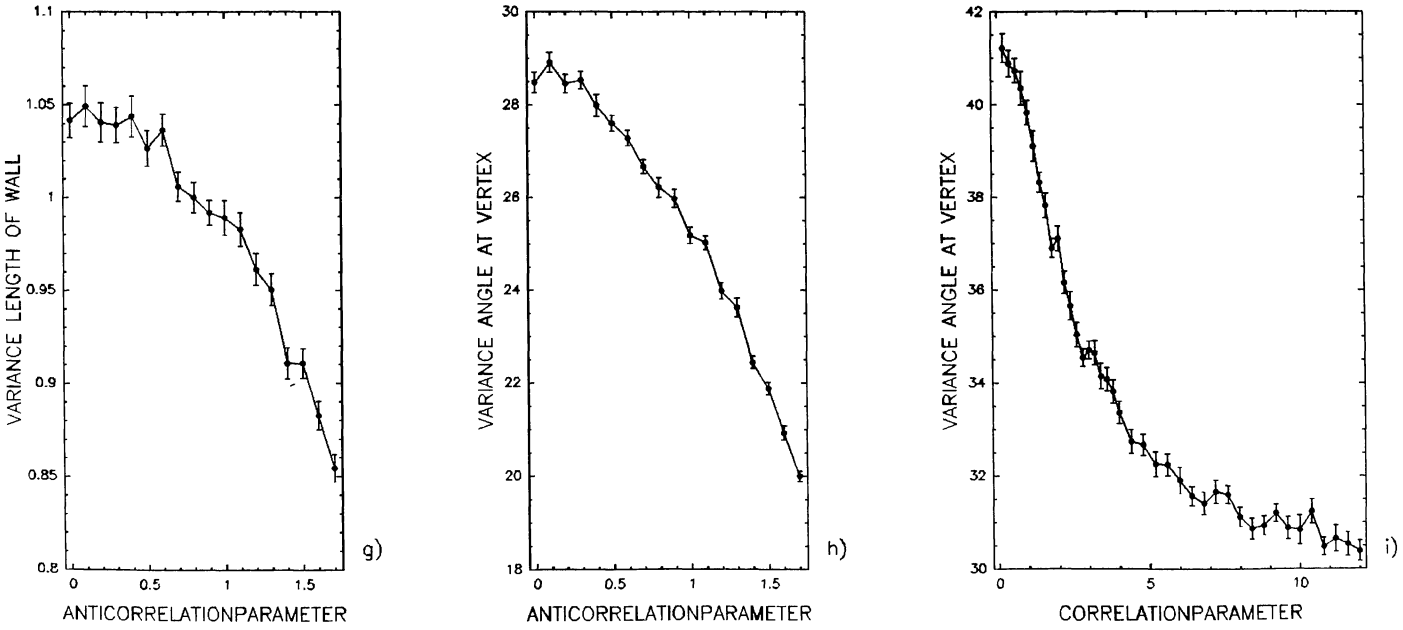

Fig. 6g–i

Apparently, the frequency distributions of a quantity for different anticorrelation parameters do resemble each other, as seen in Fig. 7a through 7g, panels A and B, where frequency distributions in quasi-poissonian ($\delta=0$) and quasi-crystalline ($\delta=1.6$–1.7) cases are shown. These distributions are seen to be centered on practically the same mean value, although the quasi-crystalline case has clearly a distribution with a smaller width and a higher peak. However, the distributions in the case of strong correlation clearly have another appearance than those of the anticorrelated cases: they peak around another mean value, they have a much larger width, and their tails can be very long. This appearance changes fast when the correlation gets weaker, and after $\lambda \gtrsim 5$ the distribution functions closely resemble those of the poissonian case, as they should. This behaviour is clearly seen in the plots of the mean and variances of the quantities a) through g) as function of the (anti)correlation parameter (Fig. 6).

Because it would be very difficult, if not impossible, to determine observationally the frequency distribution of these quantities with the accuracy needed to discriminate between the different cases of (anti)correlation, the frequency distributions are not expected to be primarily useful for comparison with galaxy counts. Therefore, we turned to the variances (Figs. 6b–e, and 6g–i). There, the situation is rather better. We think that the variance of the angles at the vertex (Fig. 6h and i) is the most useful, for three reasons: the angle is a dimensionless quantity, and therefore is independent of the distance to the cell walls, and is likely to be more immune to selection effects; the variance spans a reasonable range of about 25° between correlated and quasi-crystalline distributions of nuclei (Fig. 6i); and the variance is always at least a full factor two less than the variance that would be caused by a completely random distribution of line segments in the sky. Some observational data on the angles between filaments of galaxies exist (Binggeli, 1982; Rhee and Katgert, 1987), but a comparison with our theoretical distributions has not yet been made.

Useful limits on the variance of the vertex angle can be obtained from the following estimates. First, consider a vertex where three lines come together which are completely randomly distributed. The probability distribution of the angles between the lines is constructed by taking an arbitrary line at the vertex; let the angle between it and a second line be α, and the angle with the third line β. Then the probability densities for α and β are $P(\alpha)=P(\beta)=1/2\pi$. The joint distribution is the product of these, and because we have to restrict ourselves to the case $\alpha+\beta \leqq 2\pi$ we have to multiply this with a factor 2:

$$P(\alpha,\beta)=1/2\pi^2\,. \tag{1}$$

We easily verify that

$$\langle\alpha\rangle=\frac{1}{2\pi^2}\int_0^{2\pi}\alpha\,d\alpha\int_0^{2\pi-\alpha}d\beta=2\pi/3 \tag{2}$$

and the same for $\langle\beta\rangle$ and the third angle $\langle\gamma\rangle=\langle 2\pi-\alpha-\beta\rangle$. Furthermore, the variance of each angle is found from $\langle\beta^2\rangle-\langle\beta\rangle^2$:

$$\langle\beta^2\rangle=\frac{1}{2\pi^2}\int_0^{2\pi}d\alpha\int_0^{2\pi-\alpha}\beta^2\,d\beta=2\pi^2/3\,. \tag{3}$$

Thus, the square of the variance is $2\pi^2/9$, and the variance itself is $\pi/3\sqrt{2}=84.^{\circ}9$.

Comparison with the angle variances given in Figs. 6h and 6i shows immediately that even in the strongly correlated case, the Voronoi variance is about half the 85° corresponding to a purely random distribution of wall directions. The finding that this variance is so much smaller is primarily due to the fact that the angle in a Voronoi cell is always less than π, while in the pure random case the angle can vary from 0 to 2π. We think that this finding could – and should – be put to the test immediately. If the angle distribution as studied by Binggeli shows a variance of the order of 90°, then either the galaxy filaments do not show cell structure, or three-dimensional projection effects obscure its effects. But if the variance is markedly less than that, is seems certain that the filaments are physically connected, probably in the shape of a Voronoi foam. In other words, we urge observers to

Fig. 7a–g. Histograms of each of the properties **a** through **g** (see Sect. 3.1) for a strongly anticorrelated (quasi-crystalline) (A), quasi-Poissonian (B) and a strongly or mildly correlated (C) distribution of nuclei:

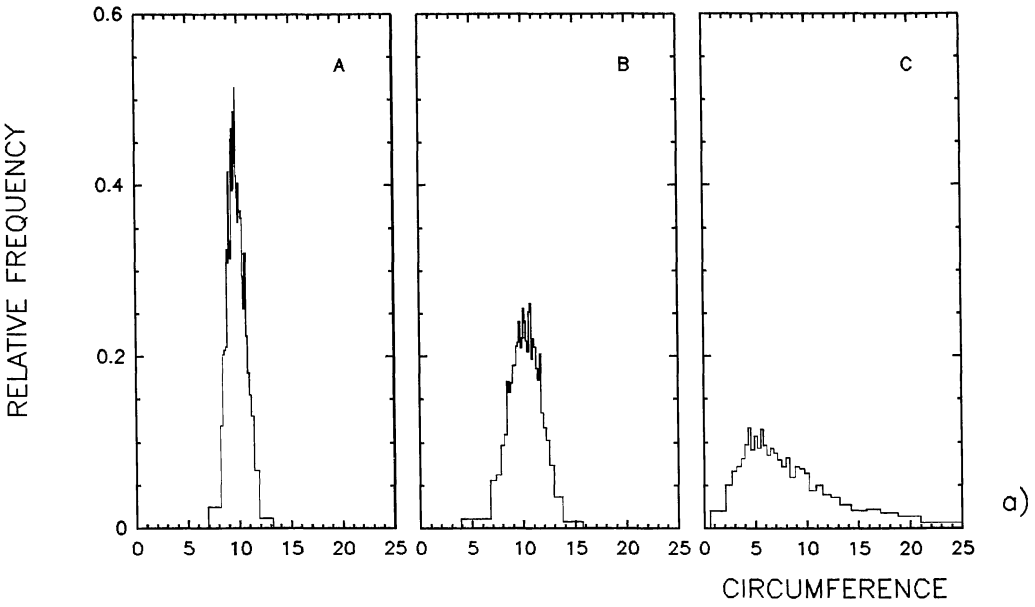

Fig. 7a. The circumference of a cell. A: $\delta = 1.7$, B: $\delta = 0.0$, C: $\lambda = 2.0$

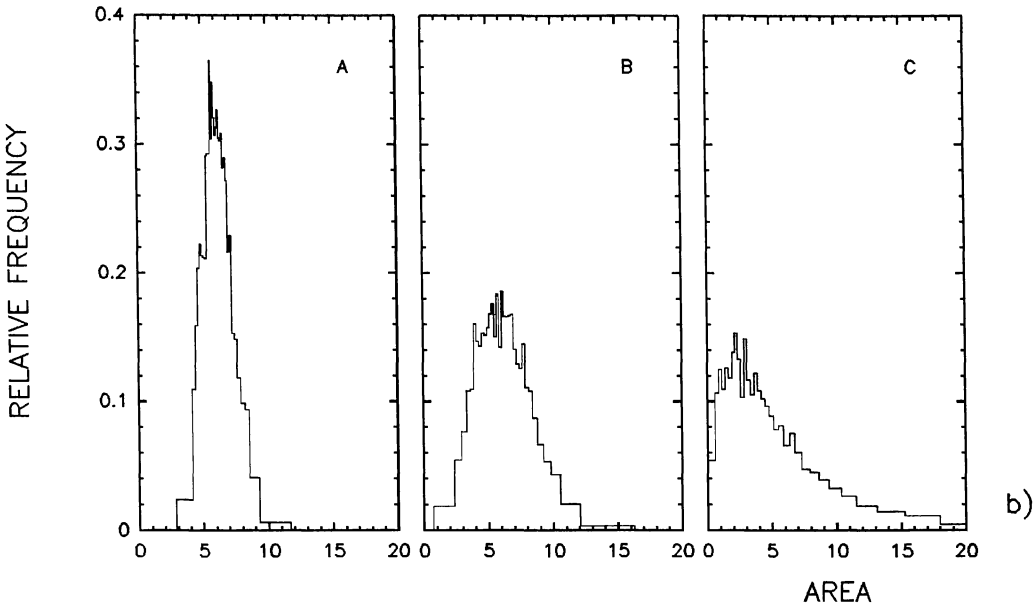

Fig. 7b. The area of a cell. A: $\delta = 1.6$, B: $\delta = 0.0$, C: $\lambda = 3.8$

consider the *variance* of the angles measured when searching for the "Binggeli effect".

The variances of the vertex angles in our two dimensional Voronoi foams range from about 42° in the case of strong correlation of the nuclei, down to roughly 30° for nuclei generated by a Poisson process. When the nuclei are strongly anticorrelated, the variance tends to zero, as expected for a crystalline distribution. The variance in the Poisson case can be exactly determined (cf. Miles, 1970). Consider an arbitrary Delaunay triangle. Because we are only interested in angles, the absolute scale of the triangle does not matter, so that we can freely pick a circumcentre and three vertices on its corresponding circumcircle (with arbitrary radius). The distances between the vertices, i.e. the lengths of the sides of the triangle, follow the Poisson distribution; because this does not contain an intrinsic length scale, the probability distributions of the sides are proportional to the lengths of these sides, so that the probability density F of finding a Delaunay triangle with sides A, B, and C is

$$F(A, B, C) \propto A\,B\,C\,. \tag{4}$$

Evidently, a side A of the Delaunay triangle is proportional to the sine of the angle opposing it (Fig. 8a and b). Thus the

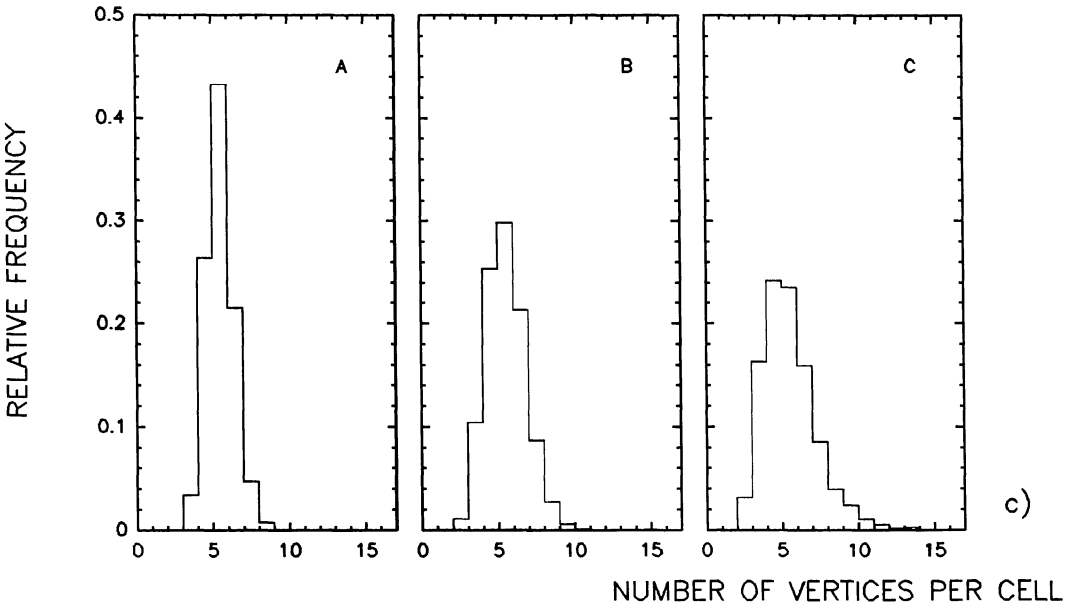

Fig. 7c. The number of vertices per cell. A: $\delta = 1.7$, B: $\delta = 0.0$, C: $\lambda = 0.2$

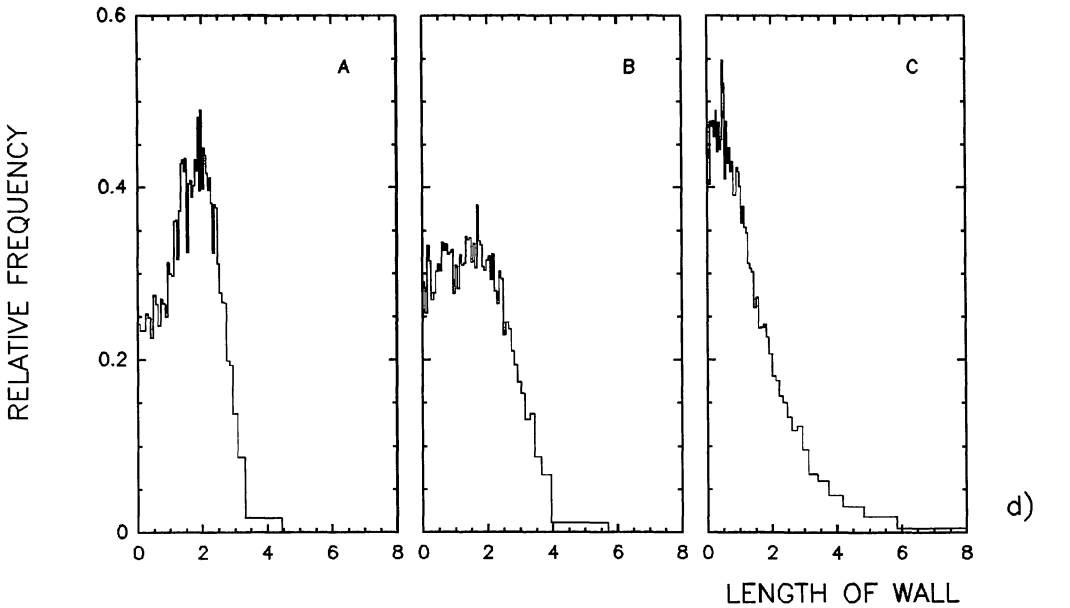

Fig. 7d. The length of a wall. A: $\delta = 1.7$, B: $\delta = 0.0$, C: $\lambda = 2.2$

probability density P_D for the distribution of the angles a, b, and c $(= \pi - a - b)$ is

$$P_D \propto \sin a \sin b \sin c \tag{5}$$

Normalization of P_D and insertion of $c = \pi - a - b$ gives (Miles, 1970)

$$P_D = \frac{8}{3\pi} \sin a \sin b \sin (a + b). \tag{6}$$

The angles α, β, and γ spanned by the Voronoi walls meeting at the circumcentre of the Delaunay triangle have, for geometrical reasons, $(a + \alpha = \pi,\ b + \beta = \pi,\ c + \gamma = \pi$, see Fig. 8a and b), a probability density P_V which is the same as P_D (apart from a minus sign):

$$P_V = -\frac{8}{3\pi} \sin \alpha \sin \beta \sin (\alpha + \beta). \tag{7}$$

$$\alpha + \beta + \gamma = 2\pi$$
$$\alpha < \pi,\ \beta < \pi,\ \gamma < \pi$$
$$\alpha + \beta > \pi. \tag{8}$$

It is straightforward to show that the expectation value and the variance of any vertex angle are

$$\langle \alpha \rangle = 2\pi/3$$
$$\langle \alpha^2 \rangle = 5\pi^2/9 - 5/6$$
$$\langle \alpha^2 \rangle - \langle \alpha \rangle^2 = \pi^2/9 - 5/6. \tag{9}$$

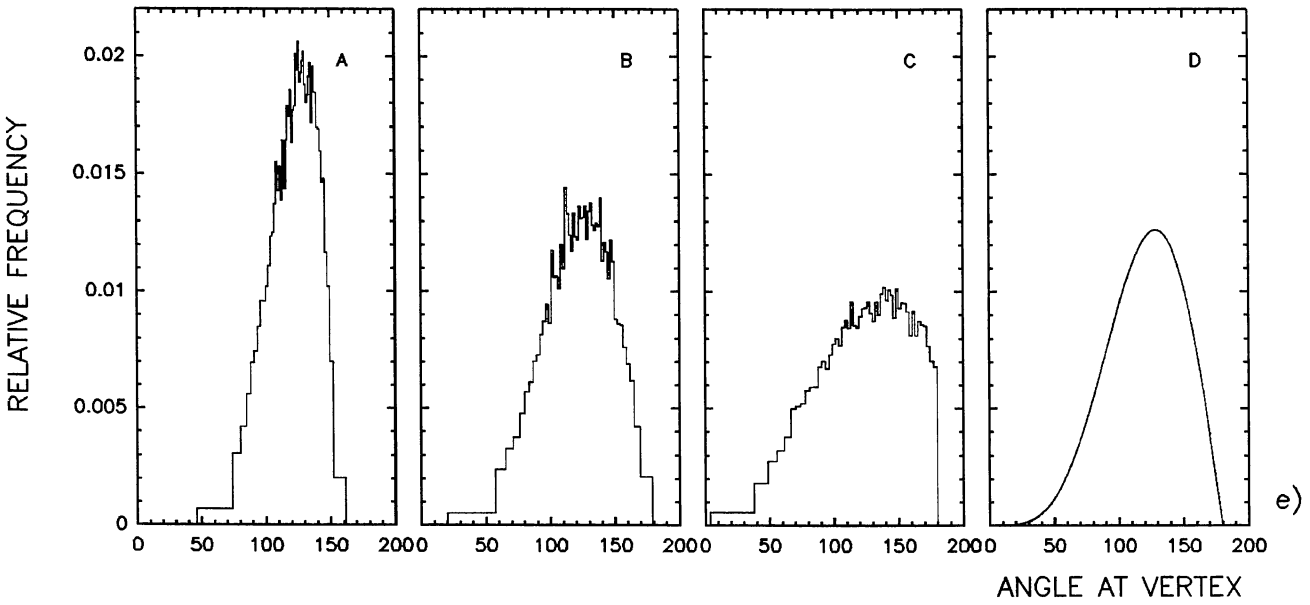

Fig. 7e. The angle at a vertex. A: $\delta = 1.7$, B: $\delta = 0.0$, C: $\lambda = 2.0$, D: theoretical distribution (Eq. (10)) for a Poissonian distribution of nuclei (see also Figs. 9 and 10)

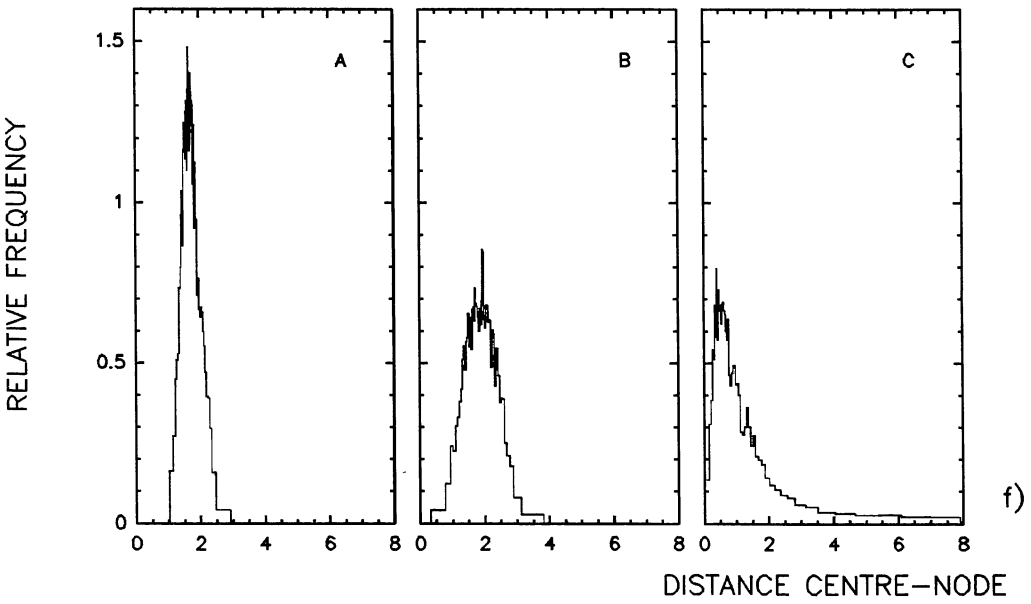

Fig. 7f. The distance centre-node. A: $\delta = 1.7$, B: $\delta = 0.0$, C: $\lambda = 1.4$

This variance, 29°.40, is the one that is observed in our Monte Carlo experiments (Fig. 6h and i). Furthermore, by integrating over β we get the distribution function $f_V(\alpha)$ for any angle α at a Voronoi vertex (Fig. 9):

$$f_V(\alpha) = \frac{4 \sin \alpha}{3\pi} \{\sin \alpha - \alpha \cos \alpha\} . \quad (10)$$

The most likely Voronoi angle, the mode of $f_V(\alpha)$, is given by the root of $\tan 2\alpha = 2\alpha\ (\alpha < \pi)$:. Its values is approximately 129°. The probability of having a Voronoi angle less than $\pi/2$ is

$$P(\alpha < \pi/2) = 1/6 . \quad (11)$$

In Fig. 10a and b this distribution function is compared with the two cases in our numerical experiments which most closely approximate a poissonian distribution (i.e. $\delta = 0.0$ and $\lambda = 12.0$); the resemblance with the analytical curve is as exact as can be expected [note that $f_V(\alpha)$ in Figs. 9 and 10 is expressed as a function of angles in degrees, and is scaled accordingly].

The variance in the case of strong correlation in much more difficult to calculate. We suspect that its value is $\sqrt{(\pi/6)} = 41°.45$, but we have not yet found a proof. However, an upper limit can be easily given. In the strongly correlated case, the Delaunay triangles that contribute most to the variance are those that have two corners very close together (at distance D, say) and one far away, producing a triangle with height H above base D (Fig. 8c). Thus, the angles at the circumcentre (i.e. one Voronoi vertex) are to first order

$$\alpha \simeq \beta \simeq \pi/2 + DH,\ \gamma \simeq \pi - 2D/H . \quad (12)$$

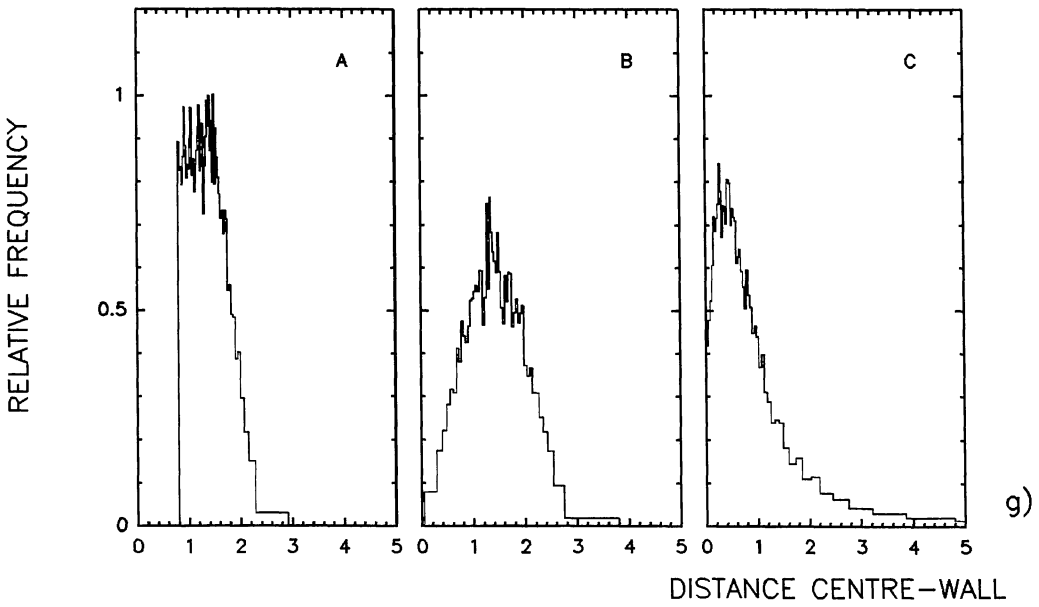

Fig. 7g. The distance centre-wall. A: $\delta = 1.7$, B: $\delta = 0.0$, C: $\lambda = 1.8$

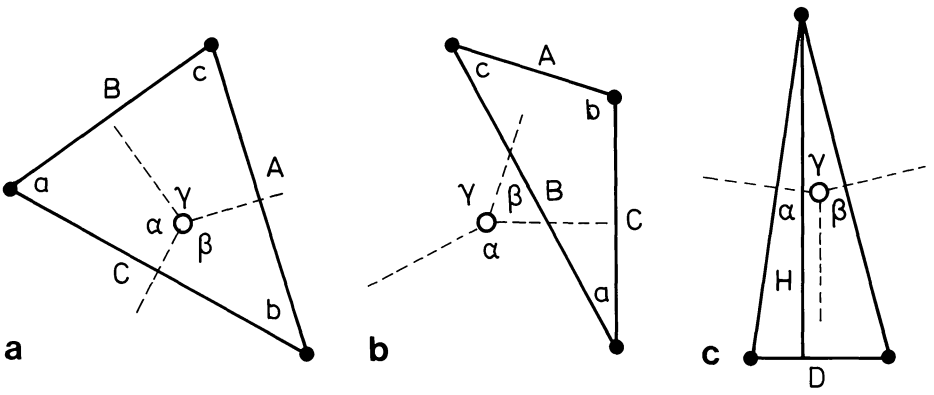

Fig. 8a–c. Plots of Delaunay triangles (solid lines), with their nuclei (filled circles) and circumcentres (open circles; these are also Voronoi vertices). Dashed lines indicate the stube of Voronoi cell walls. **a** A Delaunay triangle whose angles a, b, c are all smaller than $\pi/2$. **b** A Delaunay triangle with one angle (here b) larger than $\pi/2$; the circumcentre lies outside the triangle. Note that $\alpha + a = \beta + b = \gamma + c = \pi$, thus $\sin\alpha = \sin a$ etc. a and b are used as illustration of the derivation of Eq. (7). **c** A Delaunay triangle which contributes most to the variance of the angles at the vertices of a Voronoi cell in the case of strong correlation of nuclei [see Eq. (12)]

Since the expectation values are all $2\pi/3$, it is straightforward to show that

$$\tfrac{1}{3}(\langle\alpha^2\rangle + \langle\beta^2\rangle + \langle\gamma^2\rangle) \simeq \pi^2/18 - 2\pi D/3H, \tag{13}$$

$$\text{var} \simeq \pi/\sqrt{18} = 42.^{\circ}43 \tag{14}$$

which fits quite well with our Monte Carlo observations.

3.3. *Quantitative behaviour of the derived quantities*

We have attempted to fit the Monte Carlo results to simple functions that behave like the observed histograms, but the results were not particularly encouraging or illuminating. Thus, we refer to the accompanying figures for the quantitative results. In order to facilitate the application of our statistical model, we will publish the computer code that can be used to generate – for any distribution of nuclei – the Delaunay triangulation and the corresponding Voronoi foam.

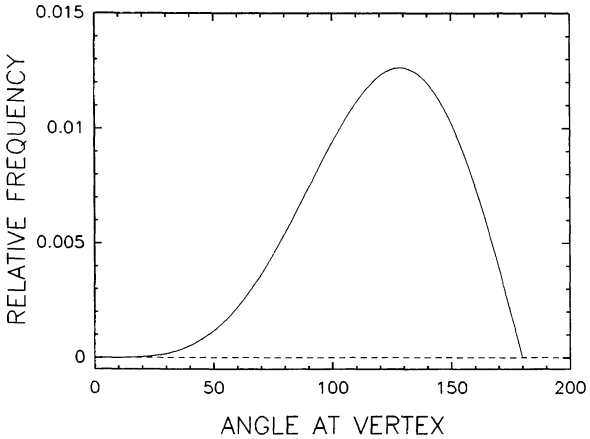

Fig. 9. The analytical distribution of the angles at vertices in a Voronoi foam with Poissonian distribution of nuclei [Eq. (10)]. Because we work with angles expressed in degrees we scaled expression (10) with a factor $\pi/180$

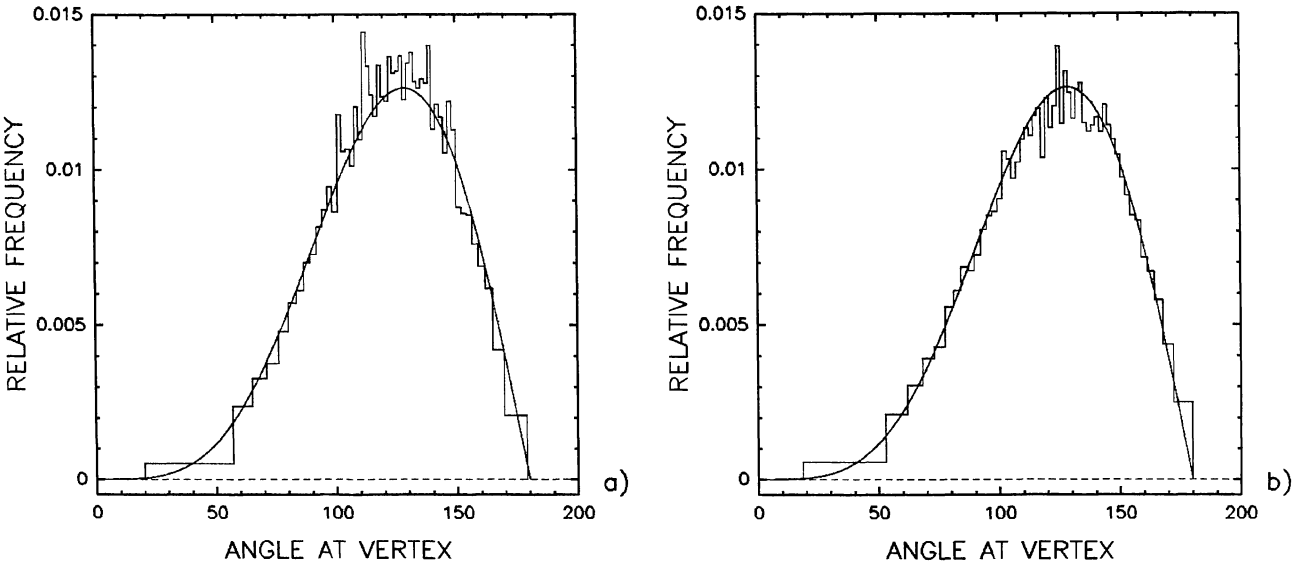

Fig. 10a and b. The analytical distribution of the angles (as in Fig. 9) compared with the two cases in our numerical computations which most resemble a poissonian distribution: **a** compared with the case of a quasi-Poissonian distribution ($\delta = 0.0$); **b** compared with the case of a very weakly correlated distribution ($\lambda = 12.0$)

4. The dynamical evolution of the voids

We have given a description of the morphology of the large scale structure of the Universe in terms of the Voronoi tessellations, which result from a spherical expansion of matter from underdense regions in the initial mass distribution. However, we have not described in detail the evolution of the matter and velocity distribution of a spherically expanding hole. In a future publication, we intend to study the formation of (1) cell walls as a consequence of the one-dimensional flow of a medium consisting of gas and (soft-particle) galaxies, (2) filaments as two-dimensional cylindrical flow, and (3) nodes as spherical inflow of the same medium.

Several authors have proposed models for the growth of underdense regions. In the pancake theory of Zel'dovich and his coworkers (Zel'dovich, 1970) voids result as a consequence of the formation of sheets where matter coalesces dissipatively in superclusters. Ostriker and Cowie (1981) and Ikeuchi (1981) suggested that spherical shock waves, generated by primordial explosive "seeds" (e.g. quasars and supernovae) would propagate outward, thereby evacuating spherical voids. But bubbles with diameters larger than 5 Mpc are difficult to make by this mechanism; it may be possible to sweep out a hole with a diameter of 50 Mpc (as seen in the observations) by assuming amplification by some kind of chain reaction of detonations (Bertschinger, 1985a) although these seed explosions have to occur very early in the Universe.

The possibility that a hole develops in the Hubble flow as a consequence of an initial deficit in the mass density was studied by Peebles (1982), Hausman et al. (1983), Hoffman et al. (1983), and Icke (1984). The latter showed explicitly that any region which is initially less dense than average will expand in such a way that it becomes more and more spherical. This effect clearly occurs in the numerical simulations carried out by Centrella and Melott (1983) and by Fujimoto (1983), who followed the nonlinear growth of a triaxial rotating underdense ellipsoid. Bertschinger (1985b) tested numerically, by a two-dimensional axisymmetric hydrodynamics code, the expansion of a nonspherical underdense region, and thereby confirmed Icke's (1984) prediction. Peebles (1982) numerically integrated the equations of motion for 2000 concentric mass shells. He finds a density profile that consists of a prominent mass ridge around a hole; the velocity field around the hole has peculiar streaming velocities which are only a small fraction of the general Hubble expansion. Hoffman et al. (1983) constructed spherically symmetric pressureless Bondi-Tolman models for hole formation in Friedmann universes, assuming a uniform initial underdensity surrounded by a compensating overdense region; they find that deep holes form even in the absence of dissipation, although the density contrasts needed at recombination to form the observed holes and rich clusters are larger than the observed limits on anisotropies in the 3 K-background would permit. Hausman et al. (1983) performed a similar study by specifying an initial spherically symmetric negative density perturbation and examining its growth and nonlinear evolution; they found choices for the initial density profile which lead to the formation of deep holes which are not surrounded by overdense shells.

Bertschinger (1983, 1985b) and Vishniac et al. (1985) recently found a general expanding self-similar solution, related to the Sedov similarlarity solution, which could be initiated by sufficiently large negative density fluctuations. Fillmore and Goldreich (1984) also derived similarity solutions, which describe the evolution of spherically symmetric voids in a perturbed Einstein – de Sitter universe filled with cold, collisionless matter. The character of a solution depends on the initial density profile, gradual perturbations giving rise to holes with smoothly rising density while steep perturbations result in voids bounded by overdense shells with sharp edges.

Analytic fluid dynamical calculations (Sato, 1982; Maeda and Sato, 1983a, b) have been applied to demonstrate that empty holes may evolve from initial perturbations of slightly subcritical density. This work was extended by Lake and Pim (1985) and Pim and Lake (1986), who studies the evolution of spherical vacuum- or radiation-filled voids in a Robertson-Walker background within the context of the general relativistic thin-wall approxi-

mation, by including background pressure, interior mass, and surface pressure. They find that voids which do not collapse grow, at late times, like the particle horizon.

These studies all clearly bear out our contention that it is easier to study the large scale structure of the Universe by looking at the evolution of the voids, because their tendency to become more spherical produces a morphological simplicity, and because their growth stays longer in the linear regime than the collapsing high-density regions. Moreover, several physical mechanisms, such as the explosion scenario of Ostriker and Cowie (1981) and Ikeuchi (1981) and the bubble theorem (Sect. 1.2), have been proposed, in which voids play a dominant role in the evolution of the large scale structure. In these models, the voids appear as real dynamical entities.

Since the luminous matter in the Universe traces the regions where the baryons are, one tends to miss the fact that most of the volume is, of course, elsewhere; this bias naturally induces resistance to the notion of using the voids as primary constituents when determining the geometry of the large scale structure. Although the reality of the sponge-like structure has not been proven beyond doubt, the discovery of large low-luminosity domains in deep radial-velocity surveys, such as the Boötes void (Kirshner et al., 1981) and the voids in the CfA survey (De Lapparent et al., 1986) make it practically impossible to argue away the existence of systematic structure on a large scale: in density, in velocity, or probably both.

5. Future work

One obvious extension of our work is, to study the properties of three dimensional Voronoi foams. This should not only provide us with a more realistic picture, but also give a check on our claim that two dimensional Voronoi foams give a fairly good description of the distribution of galaxies in the sky. The three dimensional cells will be used as the basis for our study of the dynamical evolution of the voids, and the processes taking place at the walls, filaments, and nodes.

Another improvement, albeit less essential, would be to spread the expansion centres in time and in velocity as well as in space: it is unlikely that all underdense regions were formed at exactly the same time and with the same excess Hubble parameter. However, the slowness of the subsequent evolution reduces the effect of this spread in time: if the voids start around a redshift $z \approx 10$, then the relation $t = (1+z)^{-3/2}$ indicates that the spread should be at most 1/30 of the present age of the Universe. Similarly, one might introduce a spread in the expansion rate of the voids. In all these cases, a cell wall is the locus of points where the flow travel time is the same to either nucleus. In the (degenerate) Voronoi case, this locus is a plane; in the more general cases indicated above, it is a hyperboloid, where the line between the nuclei coincides with the axis through the nuclei (Johnson and Mehl, 1939). A simple order of magnitude estimate shows that the radius of curvature at the apex of the hyperboloid is roughly equal to the distance between the nuclei, divided by the fractional deviation from equal expansion speeds. In the above case, this implies that the radius is some 30 times the internucleus distance, large enough to treat the cell walls as approximately flat.

It might be interesting to look at the possibilities of the use of Delaunay triangulation in the statistics of the galaxy distribution. Every method used to date (e.g. two point correlation, percolation, and minimal spanning) only highlights some features of the distribution; it may well be that pattern recognition methods based on Delaunay triangulation pick out some hitherto unknown properties.

An intriguing question is whether the proposed Voronoi foam structure can be seen at large redshifts. Oort (1981, 1984) considers the possibility that the Lyman α absorption lines in the spectra of quasars are connected with supercluster structures, and that they can give information on superclustering at large redshifts, assuming that the luminous matter in the Universe is largely concentrated in supercluster structures. We will simulate the correlation properties of the Lyman α lines in the spectrum of a quasar, by assuming that those lines are formed when the line of sight traverses an ensemble of hydrogen clouds distributed as a Voronoi foam. Comparing these with the observations, it might be possible to say something about clustering at early epochs.

Another possibility of applying our Voronoi tessellations is by looking at the correlation properties of the nodes in our diagrams. Because these will be the regions that attain the highest density first (where the first generation of galaxies might arise), we expect to find quasars surrounded by rich clusters in such nodes. The distribution of these objects should then be rather different from that of the filaments, as is evident in the pictures of the Voronoi foams presented here. Although Shaver (1986) concludes that the clustering scales and amplitudes of galaxy and quasar clusters are "similar", the statistics of quasar distribution is still so poor and beset by selection effects that no definitive statement can be made at present.

Acknowledgements. We are indebted to Peter Katgert and George Rhee for lively discussions, and to John Webb for advice about the observations of Lyman α clouds and for his constructive criticism of the manuscript. We are especially grateful to J.H. Oort for his constant interest and encouragement, and for his detailed assessment of earlier drafts of this work.

References

Bertschinger, E.: 1983, *Astrophys. J.* **268**, 17
Bertschinger, E.: 1985a, *Astrophys. J.* **295**, 1
Bertschinger, E.: 1985b, *Astrophys. J. Suppl.* **58**, 1
Binggeli, B.: 1982, *Astron. Astrophys.* **107**, 338
Bond, J.R., Centrella, J., Szalay, A.S., Wilson, J.R.: 1984, *Monthly Notices Roy. Astron. Soc.* **210**, 515
Brostow, W., Dussault, J.P.: 1978, *J. Comp. Phys.* **29**, 81
Burton, W.B.: 1976, *Ann. Rev. Astron. Astrophys.* **14**, 275
Centrella, J., Melott, A.L.: 1983, *Nature* **305**, 196
Centrella, J.M., Melott, A.L.: 1985, in *Numerical Astrophysics* (in honor of J.R. Wilson), eds. J.M. Centrella, J.M. LeBlanc, R.L. Bowers, p. 334
De Lapparent, V., Geller, M.J., Huchra, J.P.: 1986, *Astrophys. J. Letters* **302**, L1
De Lapparent, V., Kurtz, M.J., Geller, M.J.: 1986, *Astrophys. J.* **304**, 585
Efstathiou, G., Silk, J.: 1983, *Fund. Cosm. Phys.* **9**, 1
Einasto, J., Jôeveer, M., Saar, E.: 1980, *Monthly Notices Roy. Astron. Soc.* **193**, 353
Fillmore, J.A., Goldreich, P.: 1984, *Astrophys. J.* **281**, 9
Finney, J.L.: 1979, *J. Comp. Phys.* **32**, 137
Fischer, R.A., Miles, R.E.: 1973, *Math. Biosc.* **18**, 335
Frenk, C.S., White, S.D.M., Davis, M.: 1983, *Astrophys. J.* **271**, 9
Fujimoto, M.: 1983, *Publ. Astron. Soc. Japan* **35**, 159
Gilbert, E.N.: 1962, *Ann. Math. Stat.* **33**, 958

Gott, J.R., Melott, A.L., Dickinson, M.: 1986, *Astrophys. J.* **306**, 341
Green, P.J., Sibson, R.: 1978, *Comp. J.* **21**, 168
Hausman, M.A., Olson, D.W., Roth, B.D.: 1983, *Astrophys. J.* **270**, 351
Hoffman, G.L., Salpeter, E.E., Wasserman, I.: 1983, *Astrophys. J.* **268**, 527
Icke, V.: 1972, Ph.D. Thesis, Leiden
Icke, V.: 1973, *Astron. Astrophys.* **27**, 1
Icke, V.: 1984, *Monthly Notices Roy. Astron. Soc.* **206**, 1P
Ikeuchi, S.: 1981, *Publ. Astron. Soc. Japan* **33**, 211
Johnson, W.A., Mehl, R.F.: 1939, *Trans. Am. Inst. Min. Metal Eng.* **135**, 416
Kaiser, N.: 1987, *Monthly Notices Roy. Astron. Soc.* **227**, 1
Kendall, D.G.: 1971, *Nature* **231**, 158
Kiang, T.: 1966, *Z. Astrophys.* **64**, 433
Kirshner, R.P., Oemler, A., Schechter, P.L., Shectman, S.A.: 1981, *Astrophys. J. Letters* **248**, L57
Klypin, A.A., Shandarin, S.F.: 1983, *Monthly Notices Roy. Astron. Soc.* **204**, 891
Lake, K., Pim, R.: 1985, *Astrophys. J.* **298**, 439
Lin, C.C., Mestel, L., Shu, F.H.: 1965, *Astrophys. J.* **142**, 1431
Maeda, K., Sato, H.: 1983a, *Prog. Theor. Phys.* **70**, 772
Maeda, K., Sato, H.: 1983b, *Prog. Theor. Phys.* **70**, 1276
Melott, A.L.: 1983, *Monthly Notices Roy. Astron. Soc.* **205**, 637
Meyering, J.L.: 1953, *Philips Res. Rept.* **8**, 270
Miles, R.E.: 1970, *Math. Biosci.* **6**, 85
Miles, R.E.: 1972, *Adv. Appl. Prob. Suppl.* **4**, 243
Miles, R.E., Maillardet, R.J.: 1982, *J. Appl. Prob.*, Special Vol. **19A**, 97
Oort, J.H.: 1970, *Astron. Astrophys.* **7**, 381
Oort, J.H.: 1981, *Astron. Astrophys.* **94**, 359
Oort, J.H.: 1983, *Ann. Rev. Astron. Astrophys.* **21**, 273
Oort, J.H.: 1984, *Astron. Astrophys.* **139**, 211
Ostriker, J.P., Cowie, L.L.: 1981, *Astrophys. J. Letters* **243**, L127
Peebles, P.J.E.: 1980, *The Large Scale Structure of the Universe*, Princeton University Press
Peebles, P.J.E.: 1982, *Astrophys. J.* **257**, 438
Pim, R., Lake, K.: 1986, *Astrophys. J.* **304**, 75
Rees, M.J.: 1971, in: *Int. School Physics "E. Fermi", Course XLVII*, ed. B.K. Sachs, p. 315
Rhee, G., Katgert, P.: 1987, *Astron. Astrophys.* (in press)
Sato, H.: 1982, *Prog. Theor. Phys.* **68**, 236
Seldner, M., Siebers, B., Groth, E.J., Peebles, P.J.E.: 1977, *Astron. J.* **82**, 249
Shane, C.D., Wirtanen, C.A.: 1967, *Publ. Lick Obs.* **22**, Part 1
Shapiro, P.R., Struck-Marcell, C., Melott, A.L.: 1983, *Astrophys. J.* **275**, 413
Shaver, P.A.: 1986, *Proc. IAU Symp.* **119**, p. 475
Sibson, R.: 1980, *Scand. J. Stat.* **7**, 14
Tanemura, M., Ogawa, T., Ogita, N.: 1983, *J. Comp. Phys.* **51**, 191
Toomre, A., Toomre, J.: 1972, *Astrophys. J.* **178**, 623
Vishniac, E.T., Ostriker, J.P., Bertschinger, E.: 1985, *Astrophys. J.* **291**, 399
Voronoi, G.: 1908, *J. reine angew. Math.* **134**, 198
Zel'dovich, Y.B.: 1970, *Astron. Astrophys.* **5**, 84
Zel'dovich, Y.B., Einasto, J., Shandarin, S.F.: 1982, *Nature* **300**, 407